Journal of Sound and Vibration 329 (2010) 1007–1024

Contents lists available at ScienceDirect

Journal of Sound and Vibration

journal homepage: www.elsevier.com/locate/jsvi

Whistling of a pipe system with multiple side branches: Comparison with corrugated pipes

D. Tonon [a,*], B.J.T. Landry [a], S.P.C. Belfroid [b], J.F.H. Willems [a], G.C.J. Hofmans [a], A. Hirschberg [a]

[a] Eindhoven University of Technology, Department of Applied Physics, Fluid Dynamics Laboratory, Postbus 513, 5600 MB, Eindhoven, The Netherlands
[b] TNO Science and Industry, Postbus 155, 2600 AD, Delft, The Netherlands

ARTICLE INFO

Article history:
Received 30 April 2009
Received in revised form
26 August 2009
Accepted 14 October 2009
Handling Editor: Y. Auregan
Available online 14 November 2009

ABSTRACT

Corrugated pipes are widely used because they combine local rigidity with global flexibility. Whistling induced by flow through such pipes can lead to serious environmental and structural problems. The whistling of a multiple side branch system is compared to the whistling behavior of corrugated pipes. The study has been restricted to cavities with sharp edges which are convenient for theoretical modeling. The side branch depth is chosen to be equal to the side branch diameter, which corresponds to cavity geometries in typical corrugated pipes. The low frequency resonance modes of the multiple side branch system have been predicted by means of acoustic models, of which the validity has been tested experimentally. Several experiments have been carried out for characterizing the whistling behavior of the system. While the behavior of a multiple side branch system is interesting on its own it can be compared to that of corrugated pipes. These experiments show that the multiple side branch system is in many aspects a reasonable model for corrugated pipes. Advantage of the multiple side branch system is that it is an experimental setup allowing easy modification of cavity depth. We used this feature to identify the pressure nodes of the acoustic standing wave along the main pipe as the regions where sound is produced. This contradicts recent publications on corrugated pipes. Another interesting aspects is that the system appears to whistle at the second hydrodynamic mode of the cavities rather than at the first hydrodynamic mode. A prediction model for the whistling behavior is proposed, consisting of an energy balance, based on the vortex sound theory. The model predicts the observed Strouhal number but overestimates the acoustic fluctuation amplitude by a factor four.

1. Introduction

Corrugated pipes are used as flexible risers in offshore natural gas production systems, vacuum cleaners, ventilation systems and heat exchangers. Such pipes can display strong whistling driven by the flow through the pipe. The acoustic field produced can induce, besides environmental noise problems, significant structural vibrations. Corrugated pipes can also be used as toys or musical instruments [1–3].

Typical cross sections of corrugated pipes are shown in Fig. 1. The inner diameter oscillates periodically as we move along the pipe. The wavelength of the corrugation is called the pitch *l*. In thin wall pipes the corrugations provide the pipe

* Corresponding author. Tel.: +31 402473154; fax: +31 402464151.
E-mail address: d.tonon@tue.nl (D. Tonon).

0022-460X/$ - see front matter © 2009 Elsevier Ltd. All rights reserved.
doi:10.1016/j.jsv.2009.10.020

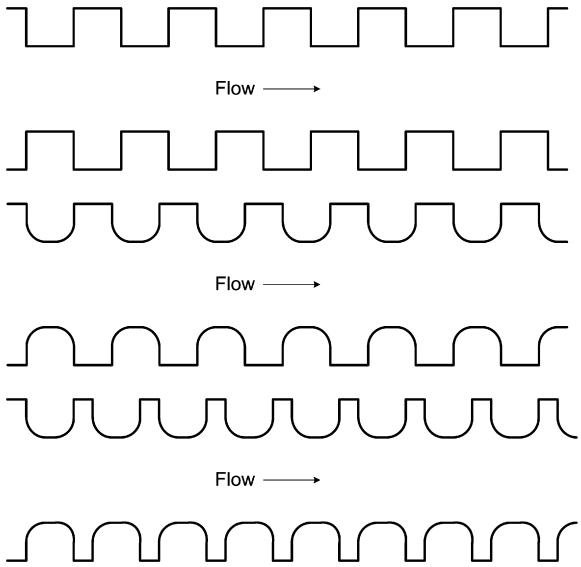

Fig. 1. Typical cross sections of corrugated pipes.

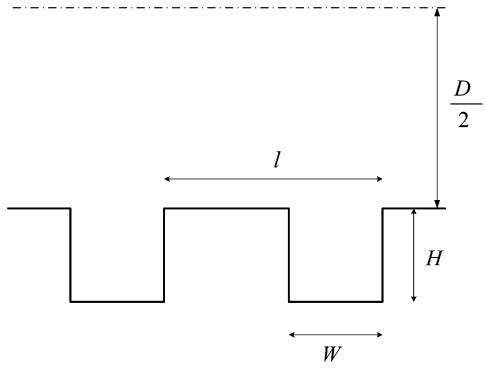

Fig. 2. Sharp edged corrugation geometry.

some local rigidity, preventing collapse, while keeping its overall flexibility. In the following we will consider the particular geometry for which the corrugation is sharp edged. The main pipe has a minimum diameter D. Each corrugation is a rectangular shaped cavity of width W in the flow direction and depth H (Fig. 2).

The flow induced whistling in corrugated pipes has been subject of several studies. From literature it appears that some characteristics of this phenomenon have been pointed out in almost all the experimental studies [1,2,4–12]. One characteristic is the stepwise increase of the whistling frequency as a function of the flow velocity. The whistling frequencies were found to be close to the acoustic resonance frequencies of the system. An interesting aspect, first observed by Cermak [4], is that the fundamental frequency is difficult to excite. It has been suggested by Cadwell [9] that this was due to the transition from laminar to turbulent flow and that whistling would only occur in turbulent flows. Another widely observed characteristic is that optimal whistling occurs at frequencies f corresponding to a critical Strouhal number $Sr_L = (fL)/U$ based on the flow velocity U and a length scale L which can either be defined based on the corrugation pitch l or on the corrugation cavity width W. Recent studies have demonstrated that the most suitable dimension to be used is the corrugation cavity width W [10,11]. When at fixed cavity width, the distance between two corrugations is increased, the critical Strouhal number $Sr_W = fW/U$ based on the cavity width does not change. This suggests that the sound production is a local fluid dynamic phenomenon within a single cavity/side branch. This is supposed to be vortex shedding triggered by the acoustic velocity fluctuation [6,8,10]. The critical Strouhal number increases according to Binnie [5] with increasing width of the cavity W relative to the pipe diameter D from $Sr_L = 0.38$ up to $Sr_L = 0.75$. Unfortunately it is not clear for the data of Binnie [5] whether the length L is chosen to be the pitch l or the cavity width W. A similar increase of critical Strouhal number has been observed by Belfroid et al. [10] when the ratio of cavity volume to pipe volume was increased.

The passive acoustic response of corrugated pipes has been described by Binnie [5] as that of a pipe with periodically placed closed side branches. Moreover he described analytically the acoustic wave behavior of the system in terms of plane waves. The model of Nederveen [13] for closed tone holes in woodwinds provides a more accurate description of the

acoustic wave behavior in the absence of main flow. For the acoustic response of a two-dimensional T-junction, Bruggeman [14] provided extensive theoretical models and experimental data. A recent detailed theoretical study of the acoustics of T-junctions has been carried out by Dubos et al. [15]. Dépollier et al. [16] studied the effect of irregularities in the depth of the side branches, which induces Anderson localization. More recently Debut et al. [17] studied numerically the effect of irregularities in the geometrical configuration on the whistling of a simplified model of corrugated pipes. A theoretical model for the acoustic wave propagation in the presence of a main flow through corrugated pipes has been proposed by Cummings, as reported by Elliot [18]. We will discuss this model more in detail later (Section 6.1).

In the present study we consider pipes with rigid walls, in that way excluding the possible coupling between flow instabilities and wall vibrations. Such a fluid–structure coupling has been observed by Ziada and Bühlmann [8] for the case of water flow through a corrugated pipe.

The hydrodynamic interaction between two successive cavities/side branches has been subject of several studies. Lange and Ronneberger [19] and Aurégan and Leroux [20] studied this interaction for the case of ducts lined with a series of equally spaced deep cavities. Ziada and Bülhmann [21] studied the hydrodynamic interaction between two side branches in close proximity. In a study of the interaction between two Helmholtz resonators, Derks and Hirschberg [22] observed that the hydrodynamic interaction becomes important for distances lower than the width of the cavity opening. In our system the distance between two successive side branches is twice the side branch width, so that we do not expect strong hydrodynamic interaction. Coupling is expected to be dominated by acoustic interaction.

The identification of the regions within the corrugated pipes where the sound is mainly produced is a matter of current debate. Kristiansen and Wiik [11] concluded that the energy generation occurs in the region of acoustic pressure antinodes and the energy absorption around the acoustic pressure nodes. They observed, however, that a short section of corrugations will only produce sound effectively when placed at the inflow end of a long smooth pipe. This position corresponds to an acoustic pressure node, which is in contradiction with their own conclusions.

There is extensive experience in our group (Fluid Dynamics Laboratory of the Department of Applied Physics, Eindhoven University of Technology) with whistling of systems of one or two closed side branches [23–27]. In particular a theoretical model based on vortex sound theory is available and has been confirmed by experiments. That was a stimulus to consider a multiple side branch system as a model for corrugated pipes, evaluating similitudes and differences between these two systems.

In this paper we first shortly introduce the theory of vortex sound and the phenomenon of self-sustained acoustic oscillations. We will explain then, using the aeroacoustic behavior of a cross configuration as example, the meaning of acoustic and hydrodynamic modes. This is followed by the description of the shear layer instability as source of unsteadiness acting as a source of sound. We will describe then the experimental setup used. This is followed by the study of the passive acoustic response of the multiple side branch system. Thereafter we will describe how the acoustic flow within a T-junction is related to the sound production. We will present then the experimental results on the whistling behavior of the multiple side branch system. We propose an energy balance to predict the critical Strouhal number for optimal whistling and the corresponding whistling amplitude. Finally we will identify the location of the regions of the multiple side branch system where the sound is produced.

To our knowledge no model predicting the whistling amplitude of corrugated pipes is available from the literature. In our model we used the acoustic source due to periodic vortex shedding as predicted by Hofmans [26]. He calculated the flow field at a T-junction by using two-dimensional incompressible frictionless flow simulations. He furthermore evaluated the sound sources applying the vortex sound theory [28] to the results of his simulations. This theory has severe limitations. Predicting the Strouhal number for whistling appears to be reasonably easy, while an accurate prediction of the whistling amplitude is not yet possible.

2. Vortex sound

A formal relationship between vortex shedding and sound generation has been established for free field conditions by Powell [29] and generalized by Howe [30,31]. Howe [31] proposes to use a Helmholtz decomposition of the flow field $\vec{u}$ to define the acoustic field:

$$\vec{u} = \nabla(\varphi_0 + \varphi') + \nabla \times \vec{\psi} \tag{1}$$

where φ_0 is a steady scalar potential, φ' is the unsteady scalar potential and $\vec{\psi}$ is the stream function. The acoustic field $\vec{u}'$ is defined as the unsteady irrotational part of the velocity field:

$$\vec{u}' = \nabla\varphi' \tag{2}$$

The ambiguity in the Helmholtz decomposition is in practice removed by the boundary conditions which we impose to the acoustic field.

We consider flows with high Reynolds number and low Mach number so that we can neglect friction and heat transfer. Assuming a homentropic flow we can use the formulation of Crocco for the momentum equation:

$$\frac{\partial \vec{u}}{\partial t} + \nabla B = -\vec{\omega} \times \vec{u} \tag{3}$$

where $B = \frac{1}{2}|\vec{u}^2| + \int \mathrm{d}p/\rho$ is the total enthalpy and $\vec{\omega} = \nabla \times \vec{u}$ is the vorticity.

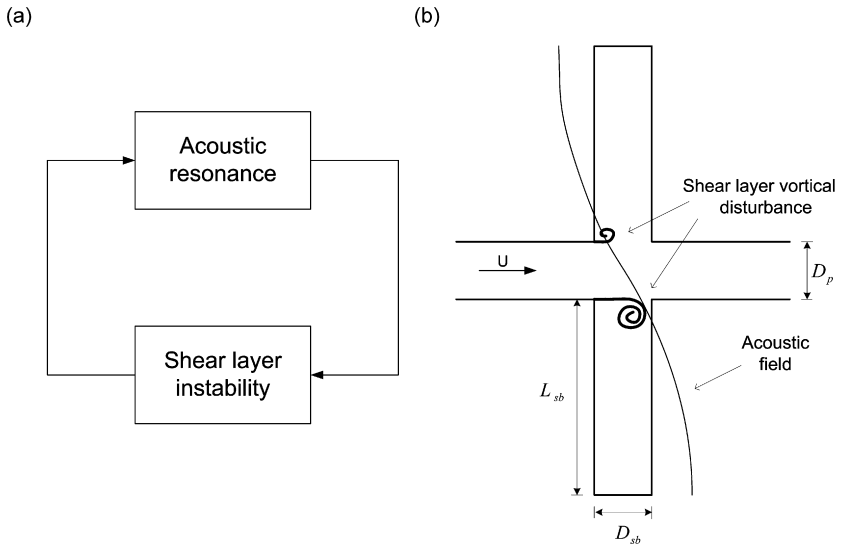

Fig. 3. Feedback loop characterizing the self-sustained oscillations (a) and double side branch system in cross configuration (b).

At low Mach numbers we can neglect the convective effects on the propagation of sound waves. With this approximation one finds

$$\frac{1}{c_0^2}\frac{\partial^2 B}{\partial t^2} - \nabla^2 B = \nabla \cdot (\vec{\omega} \times \vec{u}) \tag{4}$$

This corresponds to the assumption that the Coriolis force density $\vec{f}_{\text{coriolis}} = -\rho_0(\vec{\omega} \times \vec{u})$, where ρ_0 is the fluid density, acts as source of sound.

As proposed by Howe [31], the time-averaged acoustic source power $\langle P_{\text{source}} \rangle$ can be estimated using the approximation:

$$\langle P_{\text{source}} \rangle = -\rho_0 \left\langle \int_V (\vec{\omega} \times \vec{u}) \cdot \vec{u}' \, \mathrm{d}V \right\rangle \tag{5}$$

where V is the volume in which $\vec{\omega}$ is not vanishing and the brackets $\langle \cdots \rangle$ indicate time averaging.

The vorticity in a flow field is related to the forces acting on the flow, therefore it is related to the sound produced. One can qualitatively understand this feature by considering the tone generated by a cylinder of diameter D_{cyl} in a steady cross flow of velocity U. When we assume a potential flow around the cylinder, there is no net force applied by the flow on the cylinder because of the symmetry of the flow field. Due to viscous effects a wake is formed, vorticity shedding occurs and this breaks the symmetry. At high Reynolds numbers $Re_{D\text{cyl}} > 10^2$ instability of the wake is observed which results into periodic vortex shedding with frequency $f_{vk} = 0.2U/D_{\text{cyl}}$. This so-called von Karman vortex street [32] is associated to an oscillating lift force applied by the fluid on the cylinder. The reaction force of the cylinder to this lift force is the source of sound of the associated whistling that was studied first by Strouhal [33].

It is essential to realize that the cylinder walls do not need to vibrate in order to generate the sound. However, if a mechanical vibration of the cylinder is induced by the oscillating lift force this can significantly enhance the spatial coherence of the vortex shedding along the cylinder and result into a stronger tone with a frequency which is a compromise between the natural Strouhal vortex frequency $f_{vk}D_{\text{cyl}}/U = 0.2$ and the mechanical resonance frequency.

A similar lock-in can occur with an acoustic standing wave (resonant mode) when the cylinder is confined in a duct [34–36]. This enhances even more the sound radiation because the acoustic standing wave provides an improved radiation impedance. The resulting high amplitude oscillation controls the vortex shedding. These kinds of flow pulsations are called self-sustained oscillations. The global behavior of these oscillations can be described in terms of a feedback loop (Fig. 3a) consisting of an amplifier (flow instability) coupled to a band filter (acoustic resonance).

3. Whistling of a cross configuration

The flow induced pulsations of double side branch systems in coaxial configuration have been subject of several studies [21,24,25,27,37–39]. This configuration is obtained when two closed side branches of equal length L_{sb} and diameter D_{sb} are placed opposite to each other along a main pipe (Fig. 3b). We use the aeroacoustic behavior of this relatively simple configuration in order to introduce basic concepts such as hydrodynamic and acoustic modes.

The amplitude of the acoustic pressure measured at the top of one closed side branch $|p'_{exp}|$ and the corresponding whistling frequency f are presented as function of the main flow velocity U in Fig. 4a, as obtained by Kriesels et al. [25]. The different resonance modes, corresponding to acoustic standing waves with frequencies $f_n \cong (2n-1)c_0/(4L_{sb})$ $(n=1,2,3,\ldots)$ are clearly observed in Fig. 4a. Only the odd modes are resonant because they have a pressure node at the junction and therefore do not radiate into the main pipe.

The acoustic pressure $|p'_{exp}|$ presents distinct maxima at different critical Strouhal numbers based on the effective cavity width $Sr_{Weff} = fW_{eff}/U$. The significant Strouhal number in problems concerning the aeroacoustic behavior of pipe systems with closed side branches has been identified by Bruggeman et al. [23] to be based on the effective width of the side branches W_{eff}. For side branches with rectangular cross section, W_{eff} is equal to the width of the side branches W_{sb}, while for circular side branches of diameter D_{sb}, the effective width is the average width of the side branch cross section $W_{eff} = \pi D_{sb}/4$.

The first hydrodynamic mode $m=1$ corresponding to one vortex in the side branch opening (Fig. 4b) appears at a Strouhal number $Sr_{Weff} \cong 0.4$. The convective velocity of the vortex is about $U_{con} \cong 0.4U$ [23], hence the travel time of the vortex across the opening is one oscillation period. For the second hydrodynamic mode $m=2$ two vortices are present at the same time in the opening of the side branch (Fig. 4b), the time needed by a vortex to travel across the junction is then two oscillation periods and $Sr_{Weff} \cong 0.8$.

It appears that the sound source is the most effective when it is operating on the first hydrodynamic mode $m=1$. This mode induces pulsation amplitudes which are usually one order of magnitude larger than the pulsations induced by higher hydrodynamic modes, because it occurs at higher velocities than the higher hydrodynamic modes.

When increasing gradually the flow velocity higher order hydrodynamic modes are observed before observing the first hydrodynamic mode. In Fig. 4a we clearly observe that increasing the flow velocity the second hydrodynamic mode $m=2$ is observed for each acoustic resonance $(n=1,2,3,\ldots)$ before observing the first hydrodynamic mode $m=1$.

Self-sustained oscillations are due to instability of a feedback loop (Fig. 3a). One of the oscillation conditions determining the whistling frequency f is

$$\frac{2\pi f W_{eff}}{U_{con}} + \Delta\varphi_{ac} = 2\pi m \tag{6}$$

where $\Delta\varphi_{ac}$ is the acoustic phase shift and the first term is the phase delay due to convection. The optimal oscillation condition corresponds to acoustic resonance $f \cong f_n$ and implies in this case $\Delta\varphi_{ac} \cong 0$. By shifting the frequency f, the system can reach any phase in the range $-\pi/2 < \Delta\varphi_{ac} < \pi/2$ which allows whistling within a finite velocity range (Fig. 4a) for a given acoustic mode. However, if the resonator has a high quality factor, the frequency change is very small. We therefore observe the typical stepwise increase in frequency shown in Fig. 4a.

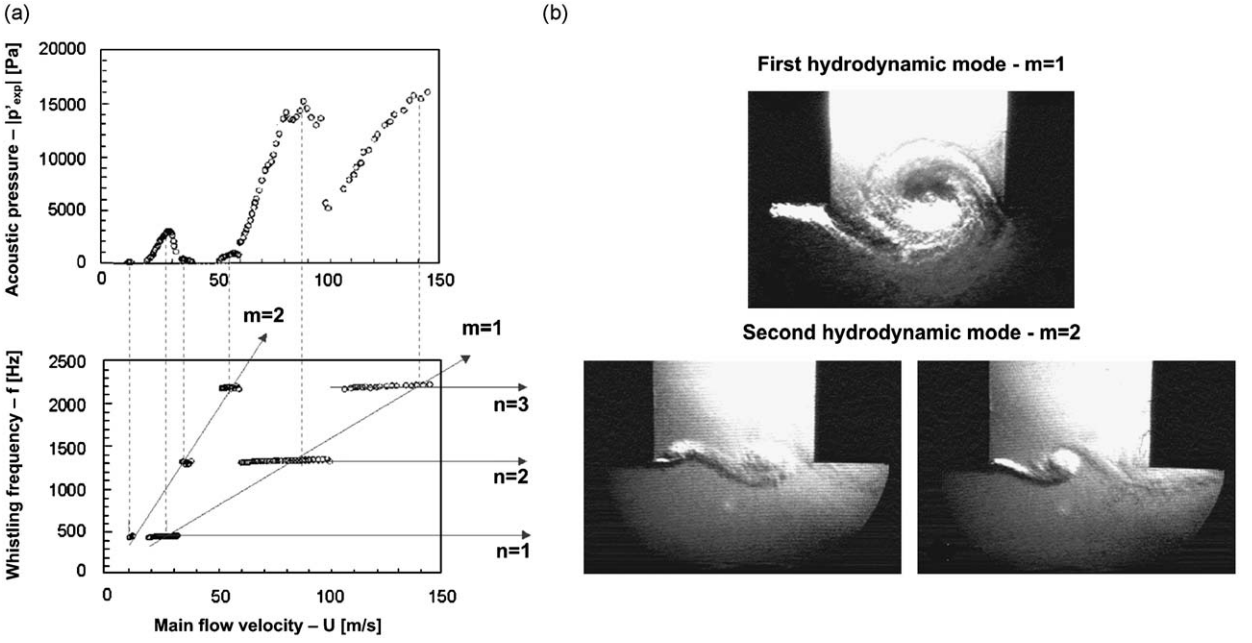

Fig. 4. Acoustic measurements [25] and flow visualizations [24] of a double side branch system in cross configuration.

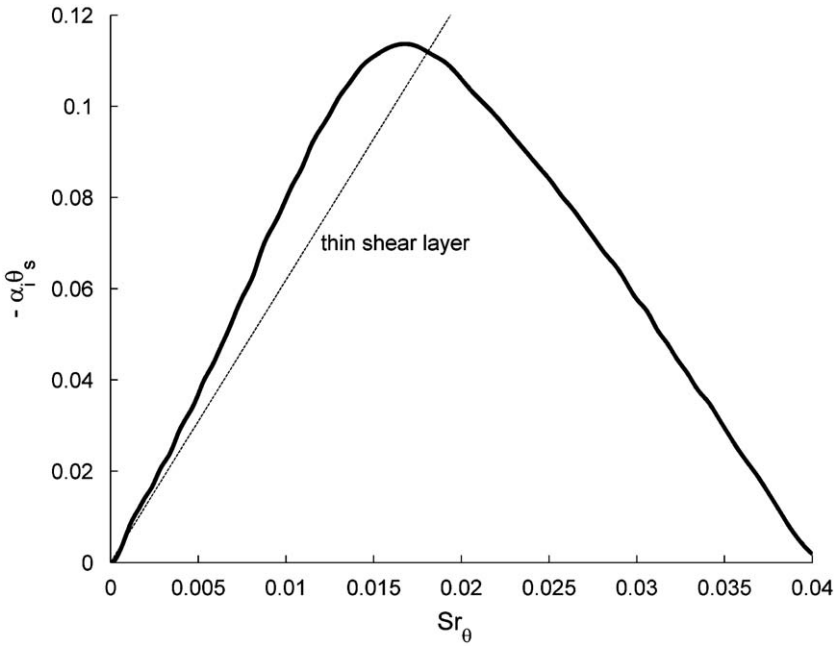

Fig. 5. Amplification rate $-\alpha_i\theta_s$ for a shear layer with finite thickness as a function of the Strouhal number based on the shear layer momentum thickness Sr_θ [41].

4. The shear layer instability

The shear layer instability is the source of unsteadiness that acts as the amplifier in the feedback loop of Fig. 3a. The growth of vortical disturbances in the shear layer that separates the main flow from the stagnant fluid has been extensively studied by means of the linearized stability theory since Rayleigh [40]. The effect of finite momentum thickness of the velocity profile of the mean flow on spatial amplification and convective velocity of hydrodynamic waves in an inviscid parallel free shear layer is described by Michalke [41]. The predicted amplification is shown as a function of the Strouhal number $f\theta_s/U$ based on the shear layer momentum thickness θ_s in Fig. 5.

For low frequencies the theory predicts an integral amplification over one wavelength by a factor $e^{2\pi}$. Furthermore the theory predicts that for frequencies above:

$$\frac{f\theta_s}{U} = 0.04 \tag{7}$$

the perturbations are not amplified. So there is no instability for hydrodynamic wavelength $\lambda_h = 0.4U/f$ shorter than about 10 times the shear layer momentum thickness θ_s.

From this theory we can conclude that when the velocity is increased monotonically the highest hydrodynamic mode to appear is determined by the critical ratio of hydrodynamic wavelength λ_h to momentum thickness θ_s discussed above.

The linear theory is correct as long as the disturbances are small. For large perturbations a roll-up of the shear layer is observed, forming coherent structures of concentrated vorticity (Fig. 4b). This concentration of the vorticity of the shear layer into discrete vortices is the nonlinear saturation mechanism which explains the stabilization of the feedback loop oscillation at a finite whistling amplitude [23,42,43].

5. Experimental setup

5.1. General setup

The experimental setup is sketched in Fig. 6. The multiple side branch system is made up of equal T-joints connected to each other, forming a row of equally spaced side branches along a main pipe (Fig. 7). The system is built up of T-junction elements for vacuum appliances *ISO-KF* cast in aluminum. The main pipe of each T-joint has an internal diameter $D_p = 33$ mm and a length $L_p = 100$ mm. The side branch is situated half-way on the main pipe segment of the T-joint. The junction between the side branch and the main pipe has sharp edges. The side branch has a diameter $D_{sb} = 33$ mm and a length $L_{sb} = 33$ mm. The end of the side branches is closed. The successive T-junctions are connected with aid of standard *ISO-KF* clamps and incorporate an O-ring for sealing. The end of each side branch is closed by means of a blank-off flange. This flange is fixed with the aid of a standard *ISO-KF* clamp and incorporates an O-ring for sealing. Plugs can be inserted

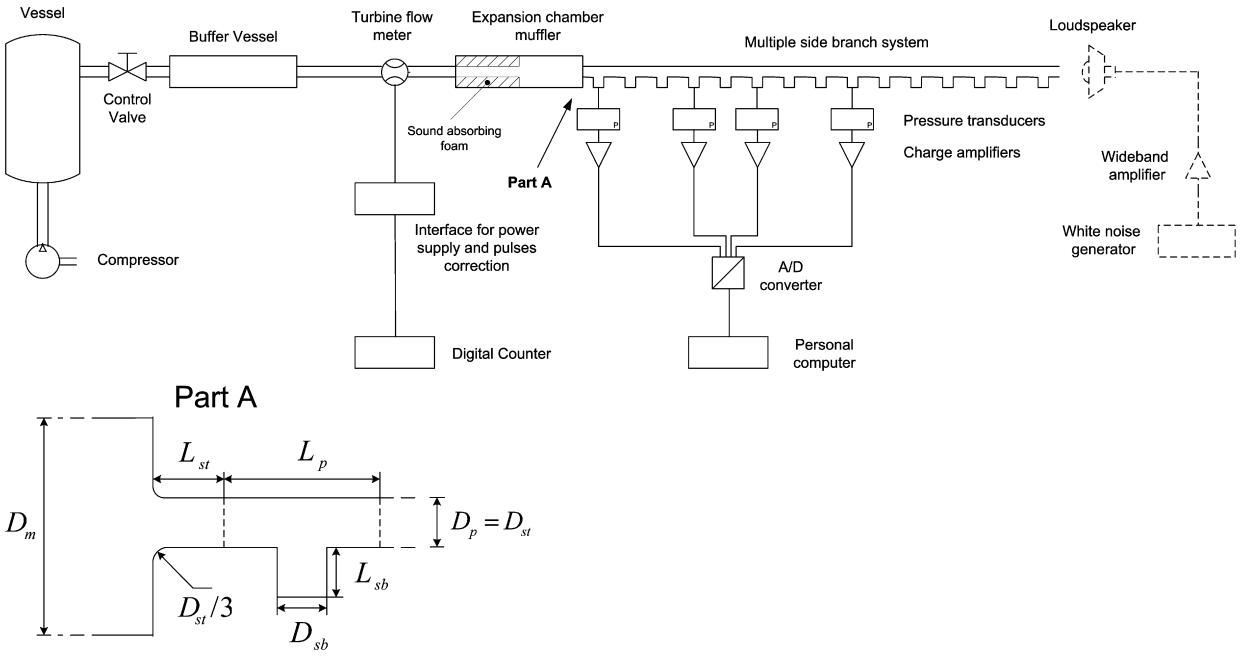

Fig. 6. Experimental setup.

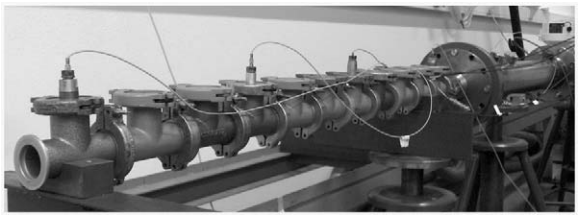

Fig. 7. Multiple side branch system.

into the side branch in order to fill up the side branch and to reduce the T-joint to a straight pipe segment. We will use these to assess the significance of specific side branches in maintaining whistling. The end walls of four side branches are supplied with flush mounted microphones.

One end of the multiple side branch system, called outlet, is open to the laboratory (a large room of 15 m × 4 m × 4 m). The other end, the inlet, is connected to a high pressure air supply system. It consists of a compressor, a 3 m^3 vessel filled with air at 15 bar, a control valve to control the flow through the system, an intermediate cylindrical buffer vessel of 1.23 m length and 20 cm diameter, a 2.3 m long pipe of 10 cm diameter, a turbine flow meter, a 1.10 m long pipe of 10 cm diameter and an expansion chamber muffler with diameter $D_m = 150$ mm and length $L_m = 930$ mm. Half of the muffler is covered internally with sound absorbing foam in order to avoid cavity resonances. Nevertheless this muffler is not ideal and appears to display around 360 Hz a resonant behavior which reduces strongly the whistling amplitudes. The multiple side branch system is connected to the muffler by a pipe segment of length $L_{st} = 41$ mm and diameter $D_{st} = 33$ mm. The upstream edge of this pipe segment has a radius of curvature of $D_{st}/3$ which avoids flow separation at the main pipe inlet.

5.2. Instrumentation

The microphones used are piezo-electric pressure transducers *PCB* 116*A*. They are linked to charge amplifiers *Kistler* 5011. These amplifiers are connected to a personal computer via an A/D converter acquisition board *National Instruments NI* cRIO-9233. The turbine flow meter *Instromet SM-RI-X-K G* 250 is used to measure the main flow velocity. It is connected to a digital counter *Systron Donner* via an interface designed in our group for the power supply of the flow meter sensor and for the correction of the pulses given by the flow meter. The temperature of the air is measured within 0.1 °C by means of a digital thermometer *Eurotherm* 91*e*. Its sensor is positioned inside the expansion chamber muffler. In order to study the passive acoustic response of the multiple side branch system we drive the acoustic field by means of a loudspeaker *Eurotec*

59-*F* 135.03-01*F* positioned 50 mm in front of the outlet of the system. The loudspeaker, used as sound source, is connected to a white noise generator *Hewlett Packard HOI*-3722*A* via an AIM wideband amplifier *WPA* 301*A*.

5.3. Geometrical comparison with a typical corrugated pipe

The geometrically relevant parameters in a corrugated pipe are: the ratio H/W of cavity depth H to cavity width W, the ratio Hf/c_0 of cavity depth H to wavelength c_0/f, the ratio l/W of pitch length l to cavity width W, the ratio W/D of cavity width W to pipe diameter D and the ratio R/W of cavity edge radius R to cavity width W. In our multiple side branch system L_{sb}/D_{sb} (corresponding to H/W in a corrugated pipe) and L_p/D_{sb} (corresponding to l/W in a corrugated pipe) are of order unity as in typical corrugated pipes. For the data presented $L_{sb}f/c_0 \ll 1$ as in corrugated pipes $Hf/c_0 \ll 1$. Concerning the ratio R/D_{sb} (corresponding to R/W in a corrugated pipe), we restricted our study to sharp edges, so $R/D_{sb} = 0$ as $R/W = 0$. Only the ratio D_{sb}/D_p (corresponding to W/D in a corrugated pipe) is in our case of order unity $D_{sb}/D_p = O(1)$ while in most corrugated pipes $W/D = O(10^{-1})$.

6. Acoustic wave propagation in the multiple side branch system

The first step of our study has been to find a simplified model for the acoustic wave propagation in the multiple side branch system without main flow. For this purpose we made use of the model proposed by Cummings as reported by Elliot [18]. We also developed a plane wave analytical model based on the low frequency plane wave acoustic model in duct segments of Dowling and Ffowcs Williams [44]. Binnie [5] had earlier proposed such a model for a multiple side branch system. We improved it by including visco-thermal damping, radiation losses and end corrections [13,14,15]. The models have been validated by comparing the theoretical predictions of both models with experimental measurements. Several experiments have been carried out for characterizing the passive acoustic behavior of the multiple side branch system.

6.1. Analytical models for wave propagation

In Cummings model, to which we will refer as "Cummings acoustic model (CAM)", the effect of the fluid in each cavity is limited to the compressibility of the cavity in which the pressure is assumed to be uniform and equal to the pressure in the main pipe [18]. The main pipe acoustic flow grazing along the cavities is assumed to be uniform. The corrugated pipe is then considered as a straight pipe presenting a side wall reactance to the acoustic field. This reactance has the effect of decreasing the effective speed of sound c_{eff} along the main pipe. Neglecting the Mach number dependency due to convective effects we find

$$c_{eff} = c_0 \frac{1}{\sqrt{1 + \dfrac{V}{Sl}}} \tag{8}$$

where c_0 is the speed of sound, V is the volume of a corrugation, S is the cross sectional area of the pipe and l is the pitch of the corrugations.

In order to use this model (CAM) for our multiple side branch system we consider the volume of a corrugation to be the volume of a single side branch $V_{sb} = \pi D_{sb}^2 L_{sb}/4$, the cross sectional area to be the cross sectional area of the main pipe $S_p = \pi D_p^2/4$ and the pitch to be the distance between two consecutive side branches L_p. The effective speed of sound c_{eff} in our multiple side branch system is then given by

$$c_{eff} = c_0 \frac{1}{\sqrt{1 + \dfrac{V_{sb}}{S_p L_p}}} \tag{9}$$

The second model, to which we will refer as "plane wave acoustic model (PWAM)", has been established by applying the continuity of mass flow and of pressure at each bifurcation and the perfect reflection condition at the side branch terminations. The resulting system of $4N$ equations with $4N+2$ unknowns, where N is the number of side branches composing the multiple side branch system, is closed mathematically by imposing two boundary conditions.

At the outlet we impose an unflanged open pipe termination and the loudspeaker is represented by an harmonically oscillating pressure discontinuity. At the inlet we impose a simple flanged open pipe termination. The fluid inside the multiple side branch system is at rest. The visco-thermal losses are taken into account as proposed by Kirchhoff [45,46]. The main pipe length is taken including the fluid at the junction. The end corrections for the side branches are taken into account by adding a correction equal to one-third of the side branch diameter $D_{sb}/3$ to the length of the side branches [14]. The more complex theory of Nederveen [13] was not implemented, because the results were already satisfactory.

Table 1
Predicted and experimental frequencies of the resonance modes of the multiple side branch system (15 side branches).

Mode number	Measured frequency, f_p	Cummings model (CAM), $\frac{\lvert f_p - f_C \rvert}{f_p} \cdot 100$	Plane wave model (PWAM), $\frac{\lvert f_p - f_{PW} \rvert}{f_p} \cdot 100$
1	89.7	3.10	1.11
2	181.3	2.02	0.22
3	271.5	2.19	0.29
4	357.7	3.42	1.28
5	454.4	1.77	0.68
6	538.1	3.12	0.20
7	621.1	4.23	0.48
8	704.8	4.98	0.42
9	784.7	6.07	0.43
10	864.8	6.94	0.06
11	927.3	9.71	0.80
12	989.2	12.19	0.85
13	1044.3	15.13	0.55

f_p is the measured frequency, f_C is the frequency predicted with the Cummings model (CAM) and f_{PW} is the frequency predicted with the plane wave model (PWAM).

6.2. Wave propagation results

The experiments to characterize the passive acoustic behavior of the multiple side branch system were performed without blowing air through the system. The loudspeaker was used as sound source. It was driven by a white noise generator with a bandwidth of 5000 Hz. Experiments have been done for a variable number of side branches and have been carried out twice: firstly with the side branch system connected to the muffler and secondly with the system disconnected from the muffler. The measured resonance frequencies were not affected by the presence of the muffler; however, around 360 Hz the amplitude of the resonance modes have been observed to be affected by the presence of the muffler. This indicates a problem which also affects the results of whistling experiments (Section 8).

The low frequency resonance modes of the multiple side branch system can be predicted by both the analytical models (CAM and PWAM). These modes correspond, for the CAM model, to standing waves with a multiple of a half-wavelength matching the pipe length:

$$L_{mp} = n\frac{c_{eff}}{2f_p} \quad (n = 1, 2, 3, \ldots) \tag{10}$$

where L_{mp} is the length of the whole main pipe and f_p is the resonance mode frequency.

Higher frequency resonance modes can be accurately predicted only by using the more complex plane wave model (PWAM). For both models (CAM and PWAM) the accuracy of the prediction increases as the number of side branches increases. For a system of 15 side branches, the resonance frequencies obtained experimentally are compared in Table 1 with the theoretical predictions of both models (CAM and PWAM). For low frequencies an accuracy of 1 percent is achieved with the plane wave model (PWAM). With the simplified model based on the effective speed of sound (CAM) we have for the first six modes about 3 percent accuracy. As expected from the earlier analysis of Binnie [5] one observes at high frequencies zones in which there is no wave propagation. Such zones are also found in periodic systems such as crystals and they correspond to forbidden energy levels in electrical conduction of solids [47]. This behavior is only predicted by the plane wave model (PWAM).

7. Acoustic flow within a T-junction and sound production

In corrugated pipes and in the multiple side branch system considered, the cavities/side branches are shallow compared to the acoustic wavelength. This implies that, in contrast with the cross configuration discussed above (Section 3), the acoustic field is not dominated by acoustic waves due to the compressibility of the cavities/side branches but it is dominated by waves traveling along the main pipe. As we will see later (Section 10), this is in agreement with the result that the sound in mainly produced at pressure nodes in the standing wave pattern along the main pipe.

Globally, we can describe the acoustic field in terms of plane waves traveling at a modified speed of sound c_{eff} along a uniform pipe (Section 6.1). Locally, however, the acoustic flow is very complex. Around the pressure nodes the acoustic flow is an oscillating potential flow grazing along a cavity. In Fig. 8a we show a sketch of the streamlines of this acoustic flow. In such a potential flow the sharp edges of the cavity are singularities at which the acoustic velocity becomes locally infinitely large. Further away from the wall the acoustic streamlines, which are initially (upstream of the upstream edge) parallel to the main pipe axis, bend around the upstream edge. In the middle of the cavity the streamlines bend back, up to be again parallel to main pipe axis. Finally they turn around the downstream edge and they end up parallel to main pipe axis (downstream of the downstream edge).

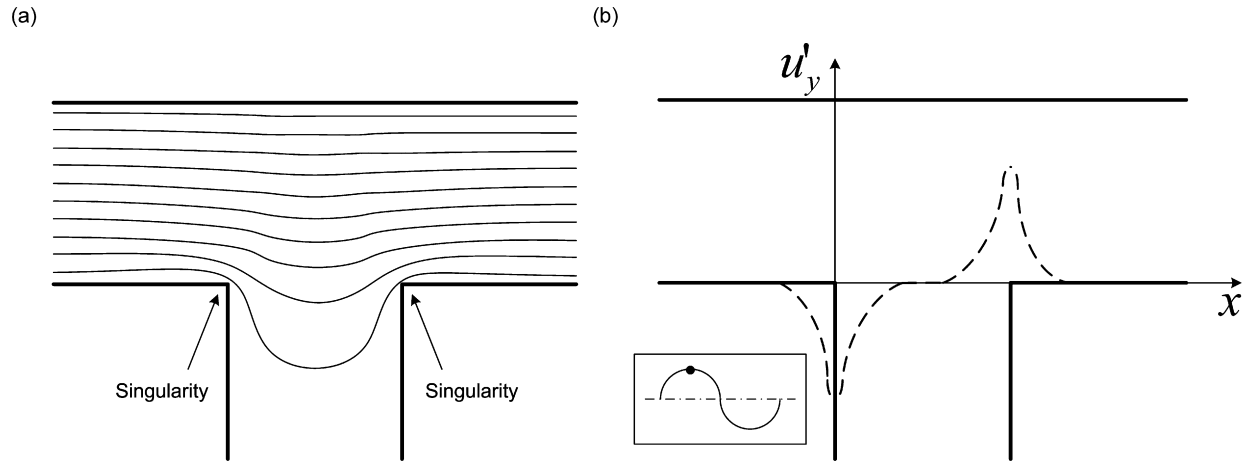

Fig. 8. Streamlines of the acoustic velocity field for the case of acoustic flow directed along the main pipe (a) and qualitative representation of the x-dependence of the vertical component of the acoustic velocity at the junction between the main pipe and the side branch (b).

The magnitude of the acoustic velocity is higher near the edges of the junction than in the middle of the cavity. As the vorticity $\vec{\omega}$ in the shear layer is mainly convected along a path corresponding to the unperturbed shear layer (straight line connecting the upstream and the downstream edges), we see from Eq. (5) that acoustic energy will be produced or dissipated around the upstream and downstream edges because the acoustic velocity $\vec{u}'$ has a large amplitude and a component directed normal to the flow velocity $\vec{u}$, so that $(\vec{\omega}\times\vec{u})\cdot\vec{u}'\neq 0$. Note that the normal component of the acoustic velocity has, for a given instant in time, near the downstream edge a sign opposite to that near the upstream edge (Fig. 8b).

As observed by Nelson et al. [48], Stokes and Welsh [49] and Bruggeman et al. [23] a new vortex is shed at the upstream edge each time the acoustic velocity changes direction in the main pipe from upstream to downstream. We choose this as the origin of time $t=0$. Since the vector $\vec{\omega}\times\vec{u}$ is directed towards the inside of the cavity, at this moment $(\vec{\omega}\times\vec{u})\cdot\vec{u}'>0$, so that sound is absorbed. The vortical perturbation generated at the upstream edge by flow separation is amplified by the shear layer instability as it is convected towards the downstream edge. It will produce sound near the downstream edge if it arrives there when the local acoustic velocity $\vec{u}'$ has a component directed outwards from the cavity. This condition is actually achieved during the first half-oscillation period after the initial vortex shedding, so for $0<t<T/2$. When the flow velocity is sufficiently large this occurs and yields the first hydrodynamic mode of the grazing acoustic flow configuration.

Assuming that the vorticity is concentrated into a point vortex growing linearly in time and convected at constant velocity along a straight line, yields the predicted acoustic source power $\langle P_{\text{source}}\rangle$ obtained by Bruggeman et al. [23] and shown in Fig. 9. In his model, Bruggeman et al. [23] consider a two-dimensional flow with side branch cross sectional area S_{sb} equal to the main pipe cross sectional area S_p. We see from this result that the optimal Strouhal number for sound production by the first hydrodynamic mode of the cavity with grazing acoustic flow is $Sr_{W\text{eff}}\cong 0.13$. The model of Bruggeman et al. [23] is not realistic because it dramatically overestimates the acoustic power generated at $Sr_{W\text{eff}}\cong 0.13$.

More realistic results are provided by the numerical calculations carried out by Hofmans [26]. In his calculations, Hofmans [26] considers a two-dimensional flow with side branch cross sectional area S_{sb} equal to the main pipe cross sectional area S_p. For a single T-joint, using the vortex sound theory of Howe [28], Hofmans [26] calculated the dimensionless time-averaged acoustic source power $\langle P_{\text{source}}\rangle/(\rho_0 U^2|u'|S_p)$ as a function of the Strouhal number based on the effective cavity width $Sr_{W\text{eff}}$ for the case of acoustic flow directed along the main pipe. The numerical simulations were performed solving the flow at a two-dimensional T-joint by means of a frictionless incompressible flow model (vortex blob method). The acoustic velocity was imposed as an oscillating boundary condition. Calculations were carried out for an acoustic velocity amplitude to main flow velocity ratio $|u'|/U=0.2$.

The results of the calculations carried out by Hofmans [26] are presented in Fig. 10. We observe here a second hydrodynamic mode around $Sr_{W\text{eff}}\cong 0.6$. Furthermore the first hydrodynamic mode is predicted for $Sr_{W\text{eff}}\leq 0.1$ and it is weaker than the second hydrodynamic mode.

It is interesting to note that the first hydrodynamic mode corresponds to only a quarter of a hydrodynamic wavelength in the cavity width. Hence, following the linear theory (Section 4), the amplification due to the hydrodynamic instability of the shear layer is only $(e^{2\pi})^{1/4}\cong 5$ for the first mode, while it is $(e^{2\pi})^{5/4}\cong 2.5\times 10^3$ for the second hydrodynamic mode. The weakness of the first hydrodynamic mode and the optimal Strouhal number $Sr_{W\text{eff}}\cong 0.6$ for the second hydrodynamic mode predicted by Hofmans [26] have been recently confirmed by the two-dimensional DNS calculations of Martínez-Lera et al. [50]. A third hydrodynamic mode is predicted around $Sr_{W\text{eff}}\cong 1.1$ but it can occur only if the shear layer is sufficiently thin to obtain a hydrodynamic instability (Eq. (7)).

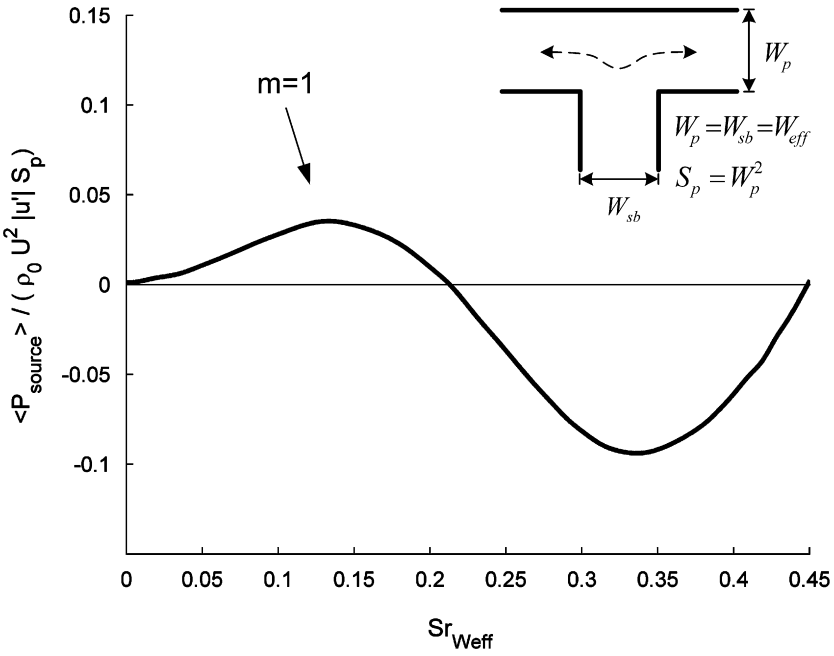

Fig. 9. Dimensionless time-averaged acoustic source power as a function of the Strouhal number based on the effective cavity width for acoustic flow directed along the main pipe. Results of the point vortex model proposed by Bruggeman et al. [23].

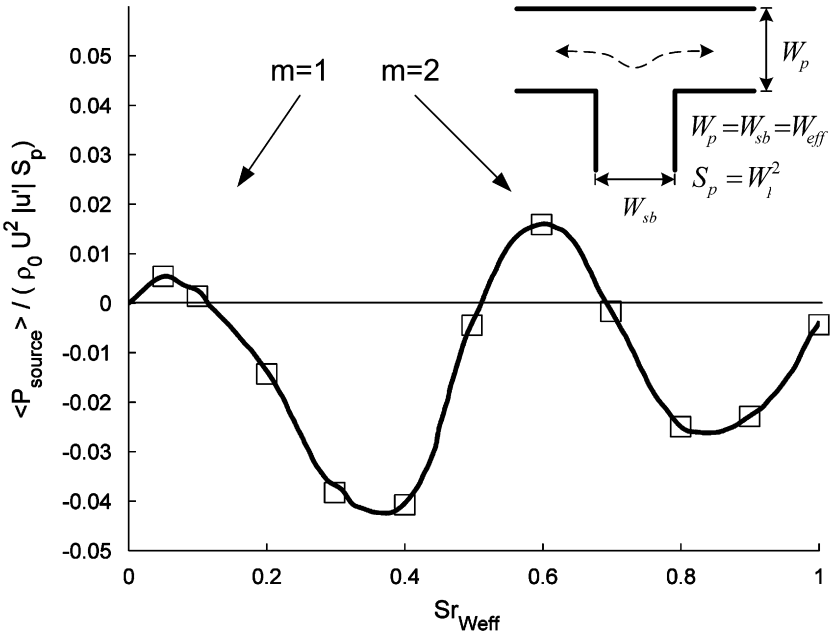

Fig. 10. Dimensionless time-averaged acoustic source power as a function of the Strouhal number based on the effective cavity width for acoustic flow directed along the main pipe. Results of the numerical simulations carried out by Hofmans [26].

8. Whistling experimental results of the multiple side branch system

When air is blown through the multiple side branch system whistling is observed. Several experiments have been carried out for a variable number of side branches.

The whistling frequency shows a stepwise increase with the flow velocity, different acoustic modes of the system being excited consecutively. The whistling frequencies observed in the experiments are close to the resonance frequencies of the

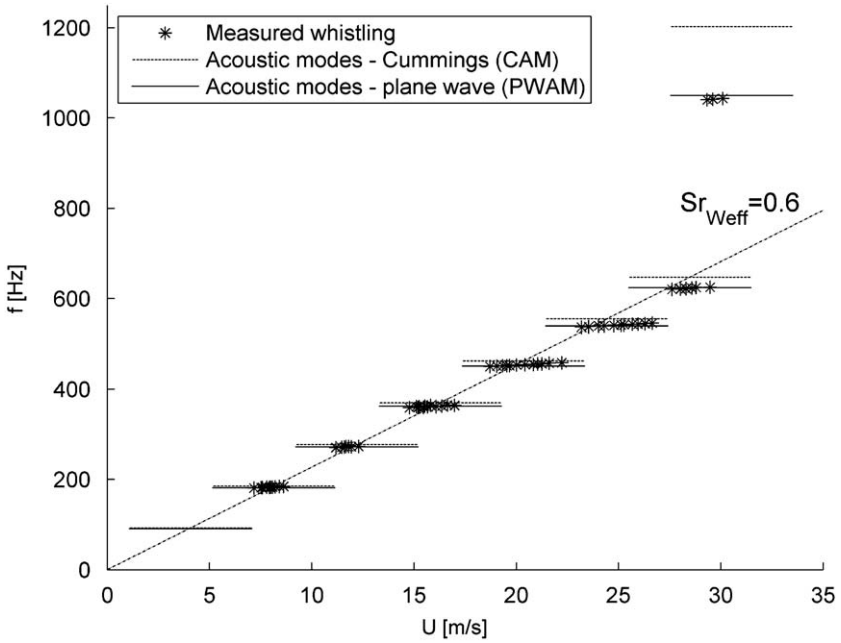

Fig. 11. Measured whistling frequency as a function of flow velocity and acoustic modes calculated by means of the analytical models (CAM and PWAM) for a system of 15 side branches.

system (Section 6). In Fig. 11 we present the measured whistling frequency f as a function of the flow velocity U for a system of 15 side branches and the acoustic modes of the system as calculated by means of the two analytical models (CAM and PWAM) presented in Section 6.1. It is interesting to note that, as often observed in corrugated pipes, whistling is absent at the lowest acoustic mode [1,2,4,5,9,11].

The flow induced whistling observed in our multiple side branch system at low velocities (below 30 m/s) occurs around a critical Strouhal number based on the effective cavity width in the range $0.5 < Sr_{W\mathrm{eff}} < 0.65$. This range corresponds to the second hydrodynamic mode of the cavity with grazing acoustic flow predicted by theory (Section 7). Furthermore we observe that upon increasing the flow velocity above 30 m/s, a hydrodynamic mode with a different Strouhal number is excited. We will focus on the range below this critical velocity.

The Strouhal critical number $Sr_{W\mathrm{eff}}$ remains almost constant when the velocity changes and when the number of side branches is changed. For whistling at the lowest excited acoustic mode, a maximum of the acoustic amplitude is found at

$$Sr_{W\mathrm{eff}} = \frac{fW_{\mathrm{eff}}}{U} = 0.6 \tag{11}$$

where f is the whistling frequency, W_{eff} is the effective cavity width and U is the flow velocity.

In typical corrugated pipes the critical Strouhal number based on the cavity width Sr_W is also almost constant. The typical values of critical Strouhal number based on the cavity width for corrugated pipes (Fig. 13, [10]) are lower than the values based on the effective cavity width for our multiple side branch system:

$$Sr_W = \frac{fW}{U} = 0.4 \tag{12}$$

This difference can be due to geometrical differences between the corrugated pipes and our multiple side branch system. In particular we expect the ratio of cavity width to pipe diameter (W/D in corrugated pipes and W_{eff}/D_p in the multiple side branch system) to be crucial. As discussed in Section 5.3 this is a geometrical parameter that is considerably different between a corrugated pipe and our multiple side branch system.

Binnie [5] carried out experiments in which he reduced the effective pipe diameter of a corrugated pipe by inserting a rod in the main pipe along the pipe axis. He observed a similar increase in critical Strouhal number from $Sr_L = 0.38$ (it is not clear whether L is the pitch l or the cavity width W) up to $Sr_L = 0.75$ as W/D was increased from $W/D = 0.46$ up to $W/D = 1.28$.

Belfroid et al. [10] carried out experiments with various corrugated pipes. In these experiments the observed critical Strouhal numbers were in the range $0.3 \le Sr_W \le 0.5$ for the second hydrodynamic mode. Furthermore, whistling was reported at very high flow speed for Strouhal around $Sr_W = 0.1$. This would correspond to the first hydrodynamic mode. However, the dimensionless amplitudes were very low and the whistling quite unstable.

One should further investigate the effect of the ratio of cavity width to shear layer momentum thickness on the critical Strouhal number. This ratio is much larger in the multiple side branch system than in typical corrugated pipes.

In Fig. 12 we present the measured dimensionless pressure fluctuation amplitude as a function of the Strouhal number based on the effective cavity width Sr_{Weff} for a system of 15 side branches. This dimensionless amplitude is defined as the amplitude of the standing pressure wave at a pressure antinode inside the main pipe $|p'_{max}|$ divided by the air density ρ_0, the speed of sound c_0 and the main flow velocity U. This dimensionless pressure fluctuation amplitude $|p'_{max}|/(\rho_0 c_0 U) = O(10^{-2})$ is of the same order of magnitude as that observed for a corrugated pipe with sharp edged corrugations, presented in Fig. 13 [10]. In this case the corrugated pipe diameter is $D = 49$ mm. The corrugation width is $W = 4$ mm. The corrugation depth is $H = 4$ mm. The pitch of the corrugations is $l = 12$ mm. The total pipe length is $L_{tot} = 3.038$ m.

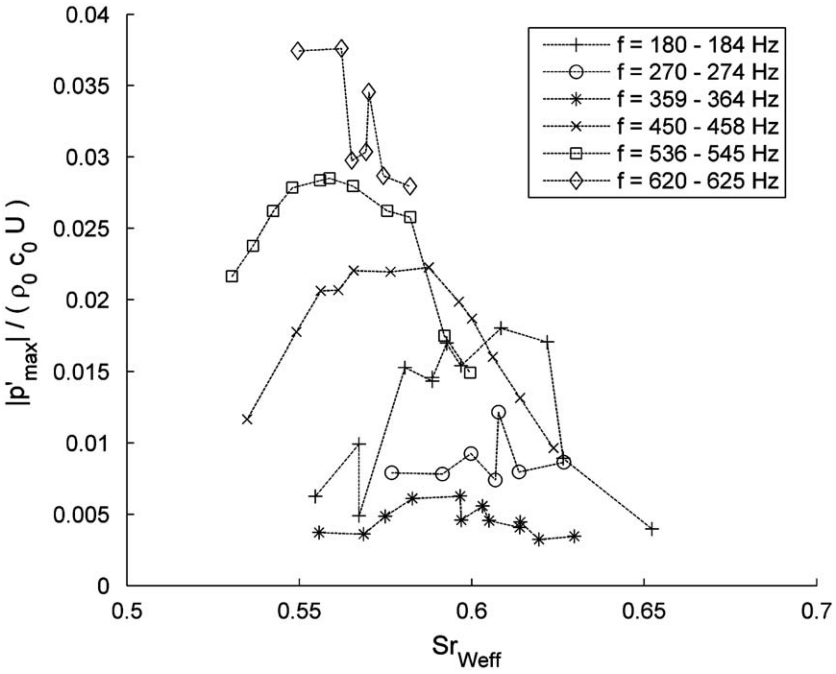

Fig. 12. Measured dimensionless pressure fluctuation amplitude as a function of Strouhal number based on the effective cavity width for a system of 15 side branches.

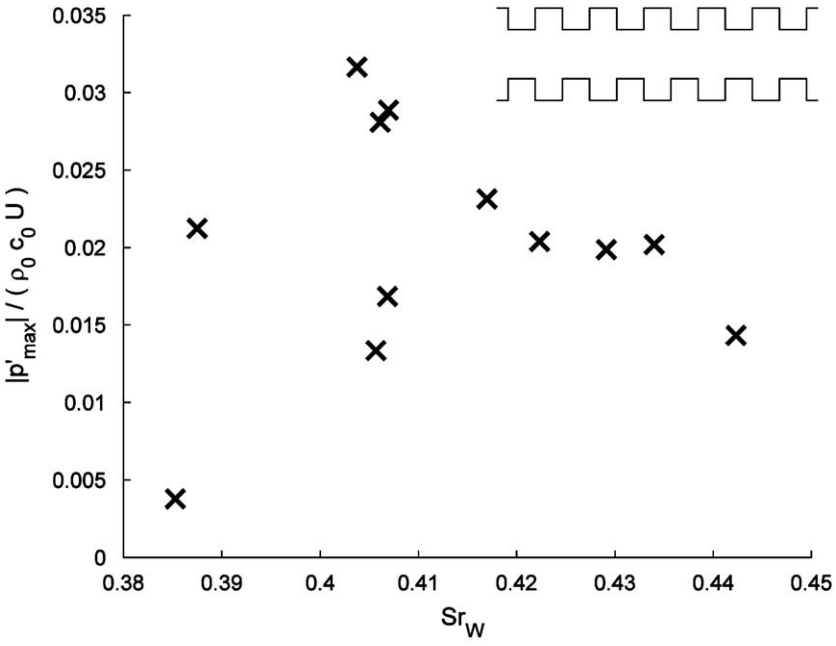

Fig. 13. Dimensionless pressure fluctuation amplitude as a function of Strouhal number based on the cavity width for a corrugated pipe with sharp edged corrugations. TNO data measured at a static pressure of 4 bar [10].

Whistling as shown in Fig. 13 [10] was obtained at a static pressure of $p_0 = 4$ bar. More details of the experimental setup and the measuring procedure are given by Belfroid et al. [10]. Note that when the edges of the corrugations are rounded Belfroid et al. [10] found dimensionless amplitudes of magnitude $|p'_{\max}|/(\rho_0 c_0 U) = O(10^{-1})$.

9. Energy balance for prediction of the whistling amplitude

As already stated in Section 4, linear theory cannot explain the occurrence of a stable whistling with finite amplitude [23,42,43]. This is a consequence of the fact that acoustic energy losses $\langle P_{\text{loss}} \rangle$ are quadratic in the acoustic amplitude $|u'|/U$. If the vorticity perturbation is linear in $|u'|/U$, the acoustic source power $\langle P_{\text{source}} \rangle$ will also be quadratic in $|u'|/U$. This implies that when $\langle P_{\text{source}} \rangle$ balances $\langle P_{\text{loss}} \rangle$ the system is neutrally stable and can have any amplitude $|u'|/U$. A very small increase in the losses is sufficient to make the system stable, killing the whistling. Therefore low amplitude oscillations are unstable. Such a behavior is indeed observed for the so-called low amplitude regime, as defined by Bruggeman et al. [23] $|u'|/U = O(10^{-3})$.

At moderate amplitudes, such as $|u'|/U = O(10^{-1})$, the shear layer vorticity is concentrated into discrete vortices [23] and becomes insensitive to the value of the acoustic amplitude. Therefore the acoustic source power $\langle P_{\text{source}} \rangle$ becomes, at a given Strouhal number, linearly proportional to $|u'|/U$. The system displays for moderate amplitudes a stable oscillation.

In our measurements we obtained whistling amplitudes of the order of $|u'|/U = O(10^{-2})$, which is intermediate between low and moderate amplitudes. This implies that it will be extremely difficult to predict the whistling amplitude. We, however, decided to make an attempt by assuming a moderate amplitude behavior. The price we have to pay for this is that we cannot predict the disappearance of a whistling mode. Our theory always predicts whistling.

The energy balance model (EBM) is a single mode model, so that the acoustic field in the multiple side branch system is considered as dominated by a single standing acoustic wave. The main idea of the model is that the acoustic source power driving this acoustic mode has to be balanced by the corresponding dissipated acoustic power. The acoustic mode considered in our model (EBM) is the first whistling mode, corresponding to a standing wave with a wavelength matching the main pipe length $f = c_{\text{eff}}/L_{\text{mp}}$.

In our prediction multiple side branch system, the wavelength of the lowest whistling modes is long compared to the side branch length. This means that the whistling is driven by the longitudinal acoustic field along the main pipe and that the component of the acoustic flow directed inside the side branches can be neglected. With this assumption, as introduced in Section 7, the acoustic source power due to vortex shedding at each side branch can be evaluated by means of the numerical simulations of Hofmans [26] (Fig. 10).

In our prediction model (EBM) we use the results of these numerical simulations, extrapolating the time-averaged acoustic source power $\langle P_{\text{source}} \rangle$ towards low amplitudes by assuming a linear relationship between $\langle P_{\text{source}} \rangle$ and $|u'|/U$ power.

Assuming this linear relationship and considering the second hydrodynamic mode, corresponding to a critical Strouhal number $Sr_{W\text{eff}} = 0.6$, we obtain for a single side branch element:

$$\frac{\langle P_{\text{source}} \rangle sb}{\rho_0 U^2 |u'| S_p} = 1.66 \times 10^{-2} = K \tag{13}$$

For the first whistling mode, the longitudinal acoustic velocity field inside the multiple side branch system is given by

$$u' = \frac{|p'_{\max}|}{\rho_0 c_{\text{eff}}} \cos\left(\frac{2\pi}{L_{\text{mp}}} x\right) \tag{14}$$

where x is the abscissa coinciding with the main pipe axis ($x = 0$ is at the main pipe inlet). This equation also defines $|p'_{\max}|$ as the pressure amplitude at a pressure antinode of the standing wave.

The time-averaged acoustic source power generated by the whole multiple side branch system at $Sr_{W\text{eff}} = 0.6$ can be then calculated by a summation of the time-averaged acoustic source power generated by each side branch:

$$\langle P_{\text{source}} \rangle = \sum_{i=1}^{N} K \rho_0 U^3 S_p \left| \cos\left(\frac{2\pi}{L_{\text{mp}}} x_i\right) \right| \frac{c_0}{c_{\text{eff}}} \frac{|p'_{\max}|}{\rho_0 c_0 U} \tag{15}$$

where x_i is the abscissa of the i-th side branch and N is the total number of side branches.

In order to satisfy the energy balance of the whole multiple side branch system the time-averaged acoustic source power has to be equal to the time-averaged acoustic losses. Losses are due to the radiation of acoustic waves, the visco-thermal dissipation (heat transfer and friction) and the vortex shedding at the open termination of the main pipe. We will consider each dissipation mechanism separately assuming that they are all independent.

For the first whistling mode considered here the radiation losses at the outlet of the system (unflanged open end) are negligible compared with the other losses. The radiated power at the inlet can be calculated from the acoustic intensity at the inlet [46]. The time-averaged acoustic power radiated is given by

$$\langle P_{\text{rad}} \rangle = S_p \langle I_{\text{inlet}} \rangle \tag{16}$$

We assume a perfect standing wave with effective speed of sound c_{eff} along the main pipe of the multiple side branch system. At resonance conditions, the longitudinal standing wave is built up of a wave traveling in the positive direction p^+

and a wave traveling in the negative direction p^-. Assuming that the sound absorbing foam in the muffler acts as an anechoic termination, the reflection coefficient for waves traveling from the main pipe inlet towards the muffler is given by

$$R_{\text{inlet}} = \frac{p^+_{\text{inlet}}}{p^-_{\text{inlet}}} = \frac{D_p^2 - D_m^2}{D_p^2 + D_m^2} \tag{17}$$

Hence the time-averaged radiation losses at the inlet are given by

$$\langle P_{\text{rad}} \rangle = \left[\frac{1}{2}(1 - R^2_{\text{inlet}})\rho_0 \frac{c_0^2}{c_{\text{eff}}} U^2 S_p\right]\left(\frac{|p^-|}{\rho_0 c_0 U}\right)^2 \cong \left[\frac{1}{8}(1 - R^2_{\text{inlet}})\rho_0 \frac{c_0^2}{c_{\text{eff}}} U^2 S_p\right]\left(\frac{|p'_{\max}|}{\rho_0 c_0 U}\right)^2 \tag{18}$$

In the last equation we assumed that the standing wave pattern is built up of a p^+ and a p^- traveling wave of almost equal amplitude, so that $p'_{\max} \cong 2p^-$.

The visco-thermal losses [46] are due to the losses inside the main pipe $\langle P_{\text{v-th } m} \rangle$ and inside each side branch $\langle P_{\text{v-th sb}} \rangle$. In order to calculate the acoustic power dissipated by the visco-thermal damping of acoustic waves in the main pipe of the system, we assume a standing wave built up of a p^+ and a p^- traveling waves of equal amplitude $p'_{\max} \cong 2p^+$. The acoustic power lost by the wave traveling in the positive direction $\langle P^+_{\text{v-th } m} \rangle$ after traveling along the whole main pipe is equal to the difference in acoustic power flow between the inlet $\langle I^+_{\text{inlet}} \rangle$ and the outlet $\langle I^+_{\text{outlet}} \rangle$. The total power loss is twice this value because we have two traveling waves of equal amplitude:

$$\langle P_{\text{v-th } m} \rangle = 2S_p[\langle I^+_{\text{inlet}} \rangle - \langle I^+_{\text{outlet}} \rangle] \tag{19}$$

The acoustic power loss by visco-thermal dissipation in the main pipe of the multiple side branch system is then given by

$$\langle P_{\text{v-th } m} \rangle = \left[2\rho_0 \frac{c_0^2}{c_{\text{eff}}} \alpha L_{\text{mp}} S_p U^2\right]\left(\frac{|p^+|}{\rho_0 c_0 U}\right)^2 \cong \left[\frac{1}{2}\rho_0 \frac{c_0^2}{c_{\text{eff}}} \alpha L_{\text{mp}} S_p U^2\right]\left(\frac{|p'_{\max}|}{\rho_0 c_0 U}\right)^2 \tag{20}$$

where α is the acoustic damping coefficient in the main pipe.

The visco-thermal losses in each side branch are calculated assuming perfect reflection at the side branch end-wall. The total power loss in each side branch is then equal to twice the power lost by the incoming wave p^+_{main} traveling along the whole side branch:

$$\langle P_{\text{v-th sb}} \rangle = 2S_{\text{sb}}[\langle I^+_{\text{main}} \rangle - \langle I^+_{\text{wall}} \rangle] = [2\rho_0 c_0 \alpha L_{\text{sb}} S_{\text{sb}} U^2]\left(\frac{|p^+_{\text{main}}|}{\rho_0 c_0 U}\right)^2 \tag{21}$$

where S_{sb} is the cross sectional area of the side branch and $\langle I^+_{\text{main}} \rangle$ and $\langle I^+_{\text{wall}} \rangle$ are the acoustic power fluxes at the main pipe section and at the end-wall, respectively. The expression of the visco-thermal losses in each side branch can be rewritten in terms of the amplitude of the standing wave inside the main pipe of the multiple side branch system $2p^+ \cong p'_{\max} \sin(2\pi x_i/L_{\text{mp}})$. The total visco-thermal losses in all the side branches is then:

$$\langle P_{\text{v-th sb}} \rangle \cong \sum_{i=1}^{N} \left[\frac{1}{2}\rho_0 c_0 \left|\sin^2\left(\frac{2\pi}{L_{\text{mp}}} x_i\right)\right| \alpha L_{\text{sb}} S_{\text{sb}} U^2\right]\left(\frac{|p'_{\max}|}{\rho_0 c_0 U}\right)^2 \tag{22}$$

where α is the acoustic damping coefficient in the side branches.

The acoustic damping coefficient α is calculated following the theory of Kirchhoff [45,46]:

$$\alpha = \frac{L_{2p}}{2S_c c_0}\sqrt{\frac{\pi f \mu}{\rho_0}}\left(1 + \frac{\gamma - 1}{\sqrt{Pr}}\right) \tag{23}$$

where L_{2p} is the perimeter of the pipe, S_c is its cross sectional area, c_0 is the speed of sound, f is the sound wave frequency, μ is the dynamic viscosity, ρ_0 is the density, $\gamma = c_p/c_v$ is the ratio of specific heat capacities and Pr is the Prandtl number.

For acoustic losses due to vortex shedding at the downstream main pipe termination we do not describe the flow in detail. We use a simpler theory, assuming a quasi-steady free jet formed at the outlet of the main pipe. According to Ingard and Singhal [51] the acoustic energy reflection coefficient is in that case:

$$\frac{\langle I^-_{\text{outlet}} \rangle}{\langle I^+_{\text{outlet}} \rangle} = \left(\frac{1 - M}{1 + M}\right)^2 \tag{24}$$

where $M = U/c_{\text{eff}}$ is the Mach number of the flow inside the main pipe of the system. The time-averaged acoustic losses due to vortex shedding at the outlet of the multiple side branch system are given by

$$\langle P_{\text{vort}} \rangle = S_p[\langle I^+_{\text{outlet}} \rangle - \langle I^-_{\text{outlet}} \rangle] = \left[\frac{1}{2}\rho_0 \frac{c_0^2}{c_{\text{eff}}} U^2 S_p\left(\frac{4M}{(1 + M)^2}\right)\right]\left(\frac{|p^+|}{\rho_0 c_0 U}\right)^2 \tag{25}$$

Assuming to be in the incompressible limit $M \ll 1$ and rewriting the expression of the vortex shedding losses in terms of the amplitude of the standing wave inside the main pipe of the multiple side branch system $p'_{\max} \cong 2p^+$ we obtain

$$\langle P_{\text{vort}} \rangle \cong \left[\frac{1}{2}\rho_0 \frac{c_0^2}{c_{\text{eff}}} U^2 S_p M\right]\left(\frac{|p'_{\max}|}{\rho_0 c_0 U}\right)^2 \tag{26}$$

In order to obtain the dimensionless amplitude $|p'_{max}|/(\rho_0 c_0 U)$ of the acoustic field inside the system, the time-averaged acoustic source power has to be balanced by the time-averaged acoustic losses:

$$\langle P_{source} \rangle = \langle P_{rad} \rangle + \langle P_{v-th\ m} \rangle + \langle P_{v-th\ sb} \rangle + \langle P_{vort} \rangle \quad (27)$$

As shown in Table 2, above 11 side branches the measured pressure fluctuation amplitude is about a factor four lower than the amplitude predicted by means of the energy balance (EBM). This difference can be explained partially by the expected deviation of our system from a two-dimensional geometry. Bruggeman et al. [23] observed, for a single side branch system with circular cross section, whistling amplitudes which were about a factor two lower than for square cross section. Moreover, the model (EBM) has been established by assuming a moderate amplitude behavior that is not expected to be accurate at the low amplitudes observed in our system. An important aspect to note is that the models for energy losses at the upstream and downstream ends of the main pipe are very crude. In particular the upstream muffler displays resonances, which significantly influence the energy balance around $f = 360$ Hz. We see from Fig. 12 that the second and the third whistling modes are weaker than the first, while our theory would predict a monotonous increase of the whistling amplitude with increasing frequency. We also see from Table 2 that upon reduction of the number of side branches the measured whistling amplitude decreases as we approach 360 Hz (Section 5). Finally the damping model does not take possible contributions from turbulence into account.

Table 2
Predicted and experimental dimensionless pressure fluctuation amplitude $|p'|/(\rho_0 c_0 U) = |u'|/U$ of the first whistling acoustic mode ($n = 2$).

Number of side branches	Whistling frequency, f	Strouhal number, Sr_{Weff}	Measured amplitude $\times 10^2$	Predicted amplitude (EBM) $\times 10^2$
8	328.1	0.60	0.47	5.34
9	293.1	0.62	0.81	5.42
10	266.7	0.61	0.76	5.58
11	245.1	0.59	1.40	5.85
12	226.7	0.58	1.90	6.10
13	210.3	0.58	1.60	6.13
14	194.7	0.60	1.46	5.99
15	183.1	0.61	1.80	6.02
16	172.1	0.61	1.55	6.25
17	161.4	0.61	1.56	6.05
18	153.8	0.60	1.56	6.16

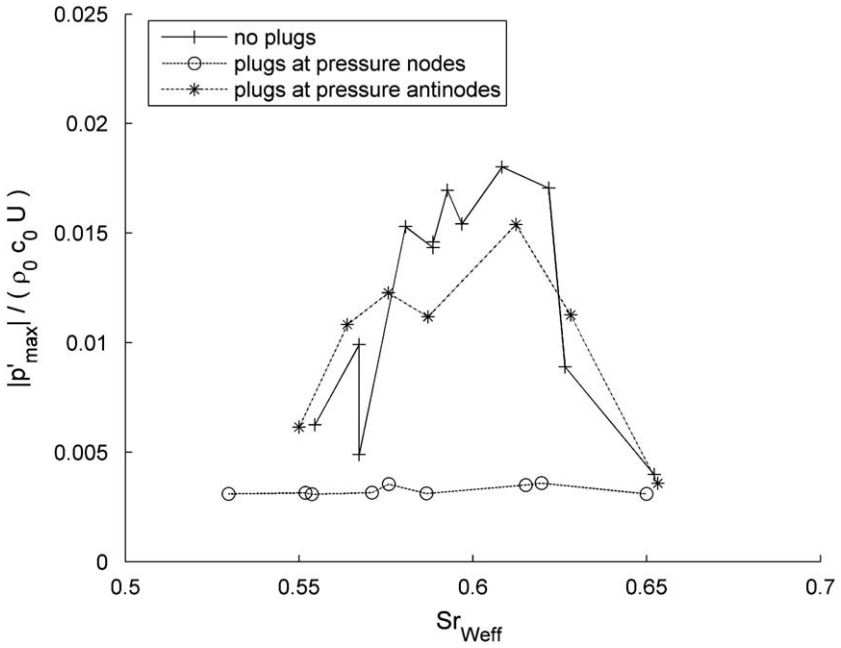

Fig. 14. Dimensionless pressure fluctuation amplitude as a function of Strouhal number based on the effective cavity width measured plugging the side branches near the pressure nodes (circles) and near the pressure antinodes (stars). System of 15 side branches.

10. Regions of sound production

The localization of the regions of the corrugated pipes where the sound is produced is a matter of current debate [11]. Our model (EBM) predicts for the multiple side branch system that the sound production is dominant within regions of high grazing acoustic velocity. These regions are located around the acoustic pressure nodes of the standing wave along the main pipe (acoustic velocity antinodes). This is confirmed by our experiments (Fig. 14) in which we consider the first whistling mode $f = c_{\mathrm{eff}}/L_{\mathrm{mp}}$. The contribution of specific side branches in our system was evaluated by plugging these side branches. As shown in Fig. 14, when the three side branches near the pressure nodes of the second acoustic mode (first whistling mode) are plugged the whistling amplitude decreases by an order of magnitude. Plugging the two side branches near the pressure antinodes only slightly affects the whistling amplitude.

11. Conclusions

In the present paper we have studied the whistling behavior of a multiple side branch systems with shallow side branches. This system is interesting by its own and it appears to have similitudes with corrugated pipes.

The great advantage of the multiple side branch system is its versatility in terms of changes in geometry, which can be obtained for instance by inserting plugs into the side branches. We used this feature in order to identify the location of the sources of sound in the system.

The low frequency resonance modes of the multiple side branch system can be predicted by assuming an effective sound propagation speed along the main pipe of the system (CAM) as proposed by Cummings [18]. The accuracy of this prediction increases as the number of side branches increases. Higher frequency resonance modes can accurately be predicted by using a plane wave model (PWAM).

A prediction model (EBM) for the whistling behavior has been proposed, which is based on the energy balance between the acoustic sources and the acoustic losses. The grazing acoustic flow is assumed to be dominant. The model does predict the observed Strouhal number $Sr_{W\mathrm{eff}} = 0.6$ but overestimates the pressure fluctuation amplitude by a factor four. One of the interesting results is that the observed whistling corresponds to the second hydrodynamic mode of the grazing flow rather than the first hydrodynamic mode.

The prediction of the amplitude is particularly difficult in a system displaying acoustic velocity fluctuations much lower than the main flow velocity as found here $|u'|/U = O(10^{-2})$. In view of the many crude assumptions used in our energy balance model (EBM), it is not surprising that the amplitude prediction is poor.

The energy balance model (EBM) predicts that the sound production occurs mainly in regions of high grazing acoustic velocity, around the pressure nodes of the standing wave along the main pipe. This is confirmed by our experiments.

Further research is now needed to assess the effect of the cavity width relative to the main pipe diameter on the critical Strouhal number reported by Binnie [5] and the effect of the ratio of cavity width to momentum thickness on the Strouhal number. We should furthermore explore the effect of rounded edges of the T-junctions. Rounding the upstream edges is expected to increase significantly the whistling amplitudes [10].

Acknowledgments

This work is being sponsored by European Commission Marie Curie RTN Project AETHER (Contract no. MRTN-CT-2006-035713). The authors wish to thank F.M.R. van Uittert, R.B.G. Balk, J. Bastiaansen and R.M.J. Tummers for their contributions to the development of the experiments and P.T. Smulders for his help in the editing of the paper.

References

[1] F.S. Crawford, Singing corrugated pipes, *Am. J. Phys.* 42 (1974) 278–288.
[2] M.P. Silverman, G.M. Cushman, Voice of the dragon: the rotating corrugated resonator, *Eur. J. Phys.* 10 (1989) 298–304.
[3] S. Serafin, J. Kojs, Computer models and compositional applications of plastic corrugated tubes, *Organised Sound* 10 (2005) 67–73.
[4] P. Cermak, Über die tonbildung bei metallschläuchen mit eingedrücktem spiralgang (On the sound generation in flexible metal hoses with spiraling grooves), *Phys. Z.* 23 (1922) 394–397.
[5] A.M. Binnie, Self-induced waves in a conduit with corrugated walls. II. Experiments with air in corrugated and finned tubes, *Proc. R. Soc. London* 262 (1961) 179–191.
[6] A.M. Petrie, I.D. Huntley, The acoustic output produced by a steady airflow through a corrugated duct, *J. Sound Vib.* 70 (1980) 1–9.
[7] Y. Nakamura, N. Fukamachi, Sound generation in corrugated tubes, *Fluid Dyn. Res.* 7 (1991) 255–261.
[8] S. Ziada, E.T. Bühlmann, Flow induced vibrations in long corrugated pipes, *International Conference on Flow-Induced Vibrations*, Brighton, 1991.
[9] L.H. Cadwell, Singing corrugated pipes revisited, *Am. J. Phys.* 62 (1994) 224–227.
[10] S.P.C. Belfroid, D.P. Shatto, R.M.C.A.M. Peters, Flow induced pulsations caused by corrugated tubes, *ASME Pressure Vessels and Piping Division Conference*, San Antonio, 2007.
[11] U.R. Kristiansen, G.A. Wiik, Experiments on sound generation in corrugated pipes with flow, *J. Acoust. Soc. Am.* 121 (2007) 1337–1344.
[12] V.F. Kopiev, M.A. Mironov, V.S. Solntseva, Aeroacoustic interaction in a corrugated duct, *Acoust. Phys.* 54 (2008) 237–243.
[13] C.J. Nederveen, *Acoustical Aspects of Woodwind Instruments*, Northern Illinois University Press, DeKalb, 1998.
[14] J.C. Bruggeman, The propagation of low-frequency sound in a two-dimensional duct system with T joints and right angle bends: theory and experiment, *J. Acoust. Soc. Am.* 82 (1987) 1045–1051.

[15] V. Dubos, J. Kergomard, A. Khettabi, J.P. Dalmont, D.H. Keefe, C.J. Nederveen, Theory of sound propagation in a duct with a branched tube using modal decomposition, *Acustica* 85 (1999) 153–169.
[16] C. Dépollier, J. Kergomard, F. Laloe, Localisation d'Anderson des ondes dans les réseaux acoustiques unidimensionnels aléatoires (Anderson localization of the waves in the acoustic one-dimensional random networks), *Ann. Phys.* 11 (1986) 457–492.
[17] V. Debut, J. Antunes, M. Moreira, Flow-acoustic interaction in corrugated pipes: time-domain simulations of experimental phenomena, *9th International Conference on Flow-Induced Vibrations*, Prague, 2008.
[18] J.W. Elliot, Corrugated pipe flow, in: M.C.M. Wrigth (Ed.), *Lecture Notes on the Mathematics of Acoustics*, Imperial College Press, London, 2005.
[19] B. Lange, D. Ronneberger, Active noise control by use of an aeroacoustic instability, *Acta Acustica United with Acustica* 89 (2003) 658–665.
[20] Y. Aurégan, M. Leroux, Experimental evidence of an instability over an impedance wall in a duct with flow, *J. Sound Vib.* 317 (2008) 432–439.
[21] S. Ziada, E.T. Bühlmann, Self-excited resonances of two side-branches in close proximity, *J. Fluids Struct.* 6 (1992) 583–601.
[22] M.M.G. Derks and A. Hirschberg, Self-sustained oscillation of the flow along Helmholtz resonators in a tandem configuration, in: E. de Langre, F. Axisa (Eds.), *Proceedings of the 8th International Conference on Flow-induced Vibration*, Ecole Polytechnique, Paris, pp. 435–440.
[23] J.C. Bruggeman, A. Hirschberg, M.E.H. van Dongen, A.P.J. Wijnands, J. Gorter, Self-sustained aero-acoustic pulsations in gas transport systems: experimental study of the influence of closed side branches, *J. Sound Vib.* 150 (1991) 371–393.
[24] M.C.A.M. Peters, Aeroacoustical Sources in Internal Flows, Ph.D. Thesis, Eindhoven University of Technology, 1993.
[25] P.C. Kriesels, M.C.A.M. Peters, A. Hirschberg, A.P.J. Wijnands, A. Iafrati, G. Riccardi, R. Piva, J.C. Bruggeman, High amplitude vortex-induced pulsations in a gas transport system, *J. Sound Vib.* 184 (1995) 343–368.
[26] G.C.J. Hofmans, Vortex Sound in Confined Flows, Ph.D. Thesis, Eindhoven University of Technology, 1998.
[27] S. Dequand, S.J. Hulshoff, A. Hirschberg, Self-sustained oscillations in a closed side branch system, *J. Sound Vib.* 265 (2003) 359–386.
[28] M.S. Howe, *Theory of Vortex Sound*, Cambridge University Press, Cambridge, 2003.
[29] A. Powell, Theory of vortex sound, *J. Acoust. Soc. Am.* 36 (1964) 177–195.
[30] M.S. Howe, Contributions to the theory of aerodynamic sound, with application to excess jet noise and the theory of the flute, *J. Fluid Mech.* 71 (1975) 625–673.
[31] M.S. Howe, The dissipation of sound at an edge, *J. Sound Vib.* 70 (1980) 407–411.
[32] P.G. Saffman, *Vortex Dynamics*, Cambridge University Press, Cambridge, 1992.
[33] V. Strouhal, Über eine besondere Art der Tonerregung, *Ann. Phys.* 241 (1878) 216–251.
[34] R.D. Blevins, *Flow-induced Vibration*, Van Nostrand Reinhold, New York, 1977.
[35] J.A. Fitzpatrick, The prediction of flow-induced noise in heat exchanger tube arrays, *J. Sound Vib.* 99 (1985) 425–435.
[36] S. Ziada, A. Oengören, E.T. Bühlmann, On acoustical resonance in tube arrays, Part I: experiments, *J. Fluids Struct.* 3 (1989) 293–314.
[37] S. Ziada, S. Shine, Strouhal numbers of flow-excited acoustic resonance of closed side branches, *J. Fluids Struct.* 13 (1999) 127–142.
[38] P.M. Radavich, A. Selamet, J.M. Novak, A computational approach for flow-acoustic in closed side branches, *J. Acoust. Soc. Am.* 109 (2001) 1343–1353.
[39] D. Arthurs, S. Ziada, Flow-excited acoustic resonances of coaxial side-branches in an annular duct, *J. Fluids Struct.* 25 (2009) 42–59.
[40] L. Rayleigh, *The Theory of Sound*, Dover Publications, New York, 1945.
[41] A. Michalke, On spatially growing disturbances in an inviscid shear layer, *J. Fluid Mech.* 23 (1965) 521–544.
[42] N.H. Fletcher, Air flow and sound generation in musical wind instruments, *Ann. Rev. Fluid Mech.* 11 (1979) 95–121.
[43] J.J. Keller, Non-linear self-excited acoustic oscillations in cavities, *J. Sound Vib.* 94 (1984) 397–409.
[44] A.P. Dowling, J.E. Ffowcs Williams, *Sound and Sources of Sound*, Ellis Horwood, Chichester, 1983.
[45] A.D. Pierce, *Acoustics*, McGraw Hill, New York, 1981.
[46] A. Hirschberg, S.W. Rienstra, Elements of aero-acoustics, *Von Karman Lecture Notes* 1994-04, Brussels, 1994.
[47] C. Kittel, *Introduction to Solid State Physics*, Wiley, Chichester, 2005.
[48] P.A. Nelson, N.A. Halliwell, P.E. Doak, Fluid dynamics of a flow excited resonance, Part I: experiment, *J. Sound Vib.* 78 (1981) 15–38.
[49] A.N. Stokes, M.C. Welsh, Flow-resonant sound interaction in a duct containing a plate, II: square leading edge, *J. Sound Vib.* 104 (1986) 55–73.
[50] P. Martínez-Lera, C. Schram, S. Föller, R. Kaess, W. Polifke, Identification of the aeroacoustic response of a low Mach number flow through a T-joint, *J. Acoust. Soc. Am.* 126 (2009) 582–586.
[51] U. Ingard, V.K. Singhal, Effect of flow on the acoustic resonance of an open-ended duct, *J. Acoust. Soc. Am.* 58 (1975) 788–793.